

AD-A248 821

TION PAGE

Form Approved  
OMB No. 0704-0188Public repc  
maintainingper response, including the time for reviewing instructions, searching existing data sources, gathering and  
Send comments regarding this burden estimate or any other aspect of this collection of information, including  
and to the Office of Management and Budget, Paperwork Reduction Project (0704-0188), Washington, DC 20503.

1. AGENCY USE ONLY (Leave blank)

2. REPORT DATE

March 1992

3. REPORT TYPE AND DATES COVERED

Professional Paper

4. TITLE AND SUBTITLE

PERFORMANCE AND AGING OF A HIGH POWER 2-D LASER DIODE ARRAY

5. FUNDING NUMBERS

PR: ZE70  
PE: 0602936N  
WU: DN308067

6. AUTHOR(S)

R. Scheps and J. Myers

7. PERFORMING ORGANIZATION NAME(S) AND ADDRESS(ES)

Naval Command, Control and Ocean Surveillance Center (NCCOSC),  
Research, Development, Test and Evaluation Division (NRaD)  
San Diego, CA 92152-50008. PERFORMING ORGANIZATION  
REPORT NUMBER

9. SPONSORING/MONITORING AGENCY NAME(S) AND ADDRESS(ES)

Office of Chief of Naval Research  
Independent Exploratory Development Programs (IED)  
OCNR-20  
Arlington, VA 2221710. SPONSORING/MONITORING  
AGENCY REPORT NUMBER

11. SUPPLEMENTARY NOTES

12a. DISTRIBUTION/AVAILABILITY STATEMENT

Approved for public release; distribution is unlimited.

DISTRIBUTION CODE

13. ABSTRACT (Maximum 200 words)

The effects of shot life on the output power, spectrum, near field, and far field patterns of a high power laser diode array have been measured and are reported, along with a description of the apparatus used to perform the measurements. The array operated for a total of  $5.9 \times 10^7$  shots at a power output equivalent to  $1 \text{ kW/cm}^2$ . A 23% degradation in output power was observed, accompanied by a 3-nm red shift of the emission maximum. The effects of the measured drop in performance are particularly relevant to the application of these devices for pumping solid state lasers.

Published in *Applied Optics*, Volume 29, No. 3, 20 January 1990.

14. SUBJECT TERMS

lasers  
solid state  
electro-optics

15. NUMBER OF PAGES

16. PRICE CODE

17. SECURITY CLASSIFICATION  
OF REPORT

UNCLASSIFIED

18. SECURITY CLASSIFICATION  
OF THIS PAGE

UNCLASSIFIED

19. SECURITY CLASSIFICATION  
OF ABSTRACT

UNCLASSIFIED

20. LIMITATION OF ABSTRACT

SAME AS REPORT

UNCLASSIFIED

21a. NAME OF RESPONSIBLE INDIVIDUAL

R. Scheps

21b. TELEPHONE (Include Area Code)

(619) 553-3730

21c. OFFICE SYMBOL

Code 843

02 4 17 087

92-09877



# Performance and aging of a high power 2-D laser diode array

Richard Scheps and Joseph Myers

The effects of shot life on the output power, spectrum, near field, and far field patterns of a high power laser diode array have been measured and are reported, along with a description of the apparatus used to perform the measurements. The array operated for a total of  $5.9 \times 10^7$  shots at a power output equivalent to  $1 \text{ kW/cm}^2$ . A 23% degradation in output power was observed, accompanied by a 3-nm red shift of the emission maximum. The effects of the measured drop in performance are particularly relevant to the application of these devices for pumping solid state lasers.

## I. Introduction

Advances in high power incoherent laser diode array technology have been dramatic in recent years. Groups working at GE,<sup>1</sup> Spectra Diode Labs,<sup>2</sup> and McDonnell-Douglas<sup>3</sup> are among those that have demonstrated array powers of the order of  $1 \text{ kW/cm}^2$  at wavelengths suitable for pumping Nd:YAG. The driving factor behind this rapid development has been the promise of efficient pumping of solid state lasers, but the effects of shot history on the output power and optical spectrum of these arrays have not been adequately detailed despite their overwhelming impact on the performance of the solid state laser. Due to the lack of detailed lifetime and aging data, unrealistic claims as to the maturity and reliability of these devices have occasionally been made and accepted. The issues associated with aging are vital for many applications, and it is to these concerns that this paper is addressed.

To this end we have assembled a laser diode array test facility capable of measuring the near field, far field, output power, electrical efficiency, and output spectrum for both pulsed and cw devices. The apparatus is computer controlled, so that measurements of the various parameters may be stored and compared with similar measurements taken after a specific number of optical pulses. The test facility design was conceived to accommodate both 1-D and 2-D arrays with output wavelengths up to  $1 \mu\text{m}$ . For pulsed diode arrays, parametric measurements may be time resolved, integrated over the entire pulse length, or

summed over any number of pulses. We have used this apparatus to record the performance of a 150-W, 2-D, 770-nm laser diode array, which is representative of arrays in this power range, and report the results below. A description of the general operation and capabilities of the test facility is also given.

## II. Test Facility

The diode array test facility has been described in detail elsewhere<sup>4</sup> and its performance is outlined briefly below. A block diagram of the apparatus is shown in Fig. 1. The system is controlled by a Hewlett-Packard HP 310 computer which coordinates timing, sequence, and IO functions. Two thirty-two-element silicon photodiode arrays are mounted on computer interfaced translation stages which move in the plane perpendicular to the laser beam axis. One of the detector arrays is mounted 2.5 cm from the laser array and is used to map the far field. The near field detector array is mounted  $\sim 1 \text{ m}$  from the array; a lens is used to image the front facet of the laser array onto the detector with a magnification of  $250\times$ . The laser diode array is mounted on a two-axis piezoelectric (PZT) driven translation stage. Both detector array outputs are routed through a sixty-four-channel scanner to an A-D converter. For cw measurements, the converter is a digital multimeter (DMM) while for pulsed measurements the converter is a transient digitizer. In either case, the output of the A-D converter is sent to the HP 310 controller for subsequent processing. The near field and far field data are acquired automatically and are stored on a hard disk for comparison with data taken after a specified number of laser pulses.

Power as a function of current is measured with an integrating sphere. The output of the sphere (cw or pulsed) is digitized and sent to the controller where it is plotted and stored. The spectral measurements may be taken several different ways, depending on the laser

The authors are with Naval Ocean Systems Center, San Diego, California 92152.

Received 7 April 1989.

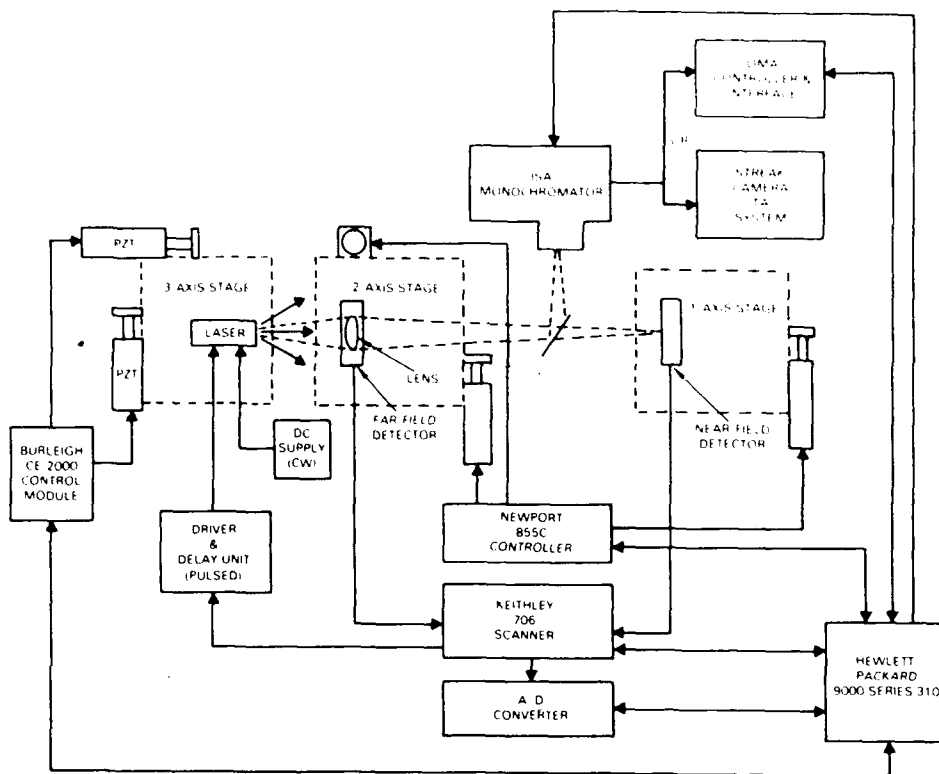


Fig. 1. Schematic diagram of the laser diode array test facility hardware.

mode of operation and the purpose of the measurement. In all cases a 0.3-m spectrometer is used. For time-resolved spectral emission, where one is concerned about the spectral shift with time during pulsed operation, a streak camera/temporal analyzer system is used. It has a minimum time resolution of 2 ps. An example of the kind of data one can obtain in this manner is shown in Fig. 2. To determine how effective a specific array is for pumping Nd:YAG it is more useful to measure the spectral emission integrated over the pulse length. This is done using a nongated optical multichannel analyzer (OMA) operating in the trigger mode. The same detector is used to measure cw array spectra. To obtain a composite spectrum of the entire array, the optical output is directed into the integrat-

ing sphere. The sphere detector is replaced with a fiber optic cable leading to the entrance slit of the spectrometer. If desired, the spectral emission of the individual laser diodes in the array can be acquired by imaging each element onto the entrance slit. The slit itself is an effective aperture for shielding the spectrometer detector from the emission of adjacent elements. The optical and mechanical systems used to image and scan the individual emitters are exactly those used for the near field measurements, with a beam splitter used to direct the near field image to the spectrometer. Scanning of the spectrometer is achieved over a GPIO bus which allows the controller to keep track of the wavelength.

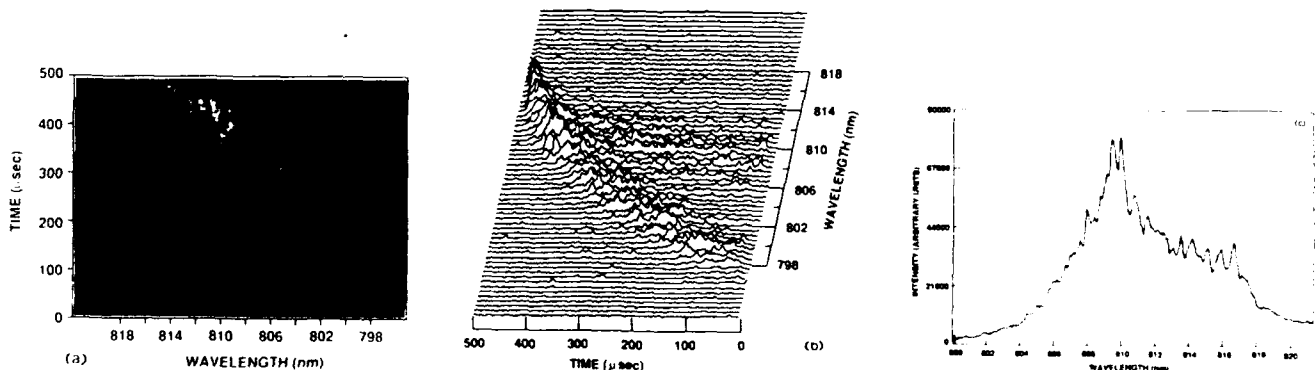


Fig. 2. (a) Streak photograph of the emission spectrum of a 1-D, 9 mm long, 810-nm laser diode array. Pulse duration is 500  $\mu$ s, peak current is 30 A, output power is 12 W, and threshold current is 14.6 A. Note that during the initial part of the pulse the junction heating is most pronounced and the spectrum red shifts rapidly, but then slowly stabilizes as the pulse continues. (b) Three-dimensional contour plot of the streak photo in (a). (c) Spectral intensity obtained from streak data integrated over the 500- $\mu$ s pulse.

The far field measurement consists of mapping the output intensity in the plane perpendicular to the laser propagation axis ( $x$ - $y$  plane) with a range of  $\pm 45^\circ$  about the central axis. With each detector element representing one pixel, the far field pattern contains 3200 pixels. The transient digitizer allocates 1000 channels of memory to each pixel in the detector array. For the 100- $\mu$ s laser pulses used in this work, the digitizer is operated with a sampling rate of 320 ns/channel, which establishes a baseline for the pulse while providing adequate temporal resolution for the optical waveform. The computer provides the triggering, scan, and timing logic for this data acquisition routine. Following the digitization of the output from the thirty-two elements in the detector array, the computer repositions the detector to map the next thirty-two pixels, continuing in this manner until all 3200 elements are recorded.

Data acquisition for the near field measurements is similar to that described for the far field. The scan routine is quite different for the near field, however, and consists of scanning both the detector and the laser diode array. Due to the high magnification, a small translation of the laser diode array using the PZT actuator produces a large shift of the image on the near field detector. Scanning the near field image then consists of scanning the detector array one pixel width (580  $\mu$ m), followed by repositioning the detector to its starting location while scanning the laser diode array to image the adjacent emitter region onto the near field detector. This sequence is repeated until the entire near field has been recorded. This scan routine avoids problems associated with the lens field of view and produces a consistently high quality image on the near field detector for all emitters independent of the overall bar length.

### III. Laser Diode Array

The laser diode array tested in this work was manufactured by GE in conjunction with the David Sarnoff Research Center and is similar to one recently described in some detail.<sup>5</sup> The specific device tested was a 2-D unphased GaAlAs array rated at 150 W peak power and operating at a nominal wavelength of 770 nm. The array area is 0.088 cm<sup>2</sup> and contains ten bars, each 4.8 mm long and having thirty-two emitters. The array was designed to pump a promethium laser and was one of several delivered to Lawrence Livermore Laboratory for that purpose. In spite of its short wavelength, we have found this array to perform as well as arrays designed to pump Nd:YAG.

### IV. Results

The diode array had in excess of  $10^7$  pulses prior to receipt, so that the aging measured did not represent initial maturation of the device. The approach taken was to perform an initial characterization of the array, followed by subsequent characterizations after  $3.6 \times 10^6$  and  $5.9 \times 10^7$  shots. The shots were accumulated while the array output power was monitored with an integrating sphere to detect the gradual fall off in

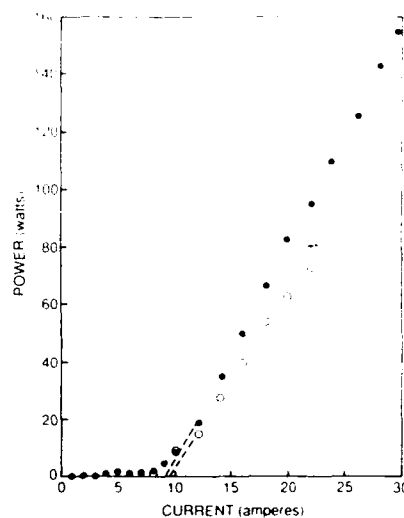


Fig. 3. Output power as a function of current for the array on receipt (●) and after  $5.9 \times 10^7$  shots (○).

performance. The array was driven with 20-A, 100- $\mu$ s pulses at duty factors between 0.2 and 0.5%. The diode array was not actively cooled. Unless otherwise noted, all the results presented below were obtained in these operating conditions.

The power as a function of current was measured several times throughout the test, and curves are shown in Fig. 3 which were taken at the start of the testing and after  $5.9 \times 10^7$  shots. Since pulse accumulation was performed at a fixed current, the output power dropped as the shot count increased. It can be seen that the legacy of the number of shots on the device performance is to lower the slope efficiency and to increase the laser threshold. The drop in electrical efficiency is accompanied by an increase in junction temperature which in turn results in a red shift of the emission spectrum. This is shown in Fig. 4 where the composite time-integrated emission peak is seen to shift  $\sim 3$  nm to the red between the start of testing and  $5.9 \times 10^7$  shots. One could mitigate this shift with active cooling. The FWHM of the emission spectrum decreased from 3.6 to 3.1 nm over the course of the testing. Note that the spectral peaks shown in Fig. 4 are not symmetric about the emission maxima, and the two curve shapes are dissimilar. The latter feature indicates that the central wavelength of each stripe does not shift uniformly, a point to which we will return.

Two far field emission patterns are shown in Fig. 5 for data taken at the start of the test and after  $3.6 \times 10^6$  shots. The orientation of the diode junctions is parallel to the  $x$ -axis, and virtually no change in the far field emission could be detected over the course of these tests. Above and to the right of each figure are plotted traces of the intensity along the  $y = 0$  and  $x = 0$  axes, respectively, which show the beam divergence about the central point in the field. The position at which the trace crosses the axis represents the 50% intensity point, and it can be seen that the full angle divergence

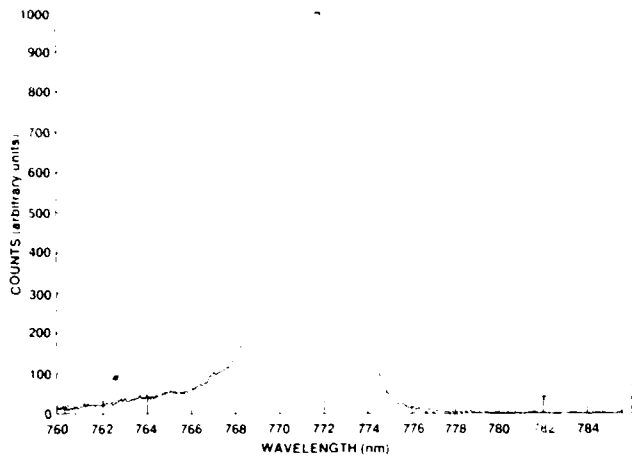


Fig. 4. Spectral emission from the laser diode array on receipt (solid) and after  $5.9 \times 10^7$  shots (dotted). Spectral data shown are the composite emission from all the stripes in the 2-D array.

is  $13^\circ$  in the plane parallel to the junction and  $45^\circ$  in the perpendicular plane. Representative near field data are shown in Fig. 6 for one bar taken after  $3.6 \times 10^6$  and  $5.9 \times 10^7$  shots. Each spike represents a separate emitting mesa region, and the uniformity across the bar is fairly good. The intensity variation from stripe to stripe seen in this bar is typical of that seen in the other nine bars. The near field trace is composed of  $\sim 3600$  points and, using software control, any specific region of the near field can be expanded graphically to a magnification consistent with the spatial resolution of  $2.3 \mu\text{m}$ . An example of this is shown in Fig. 7.

### V. Discussion and Summary

From the data it can be concluded that the major impact of aging on the array performance is to reduce the electrical efficiency and consequently red shift the peak of the emission spectrum. The near field and far field patterns are found to be substantially unaffected by shot life. The measured spectral shift is due to thermal effects and with active, regulated cooling it can be mitigated. However, the overall degradation of the output power is only counteracted with higher drive current. Maintaining constant power in this fashion will cause additional spectral shifting and possibly accelerate degradation of the array output power with shot life.

Without detailed information as to the structure of the single quantum well laser diodes it is not possible to accurately determine if the magnitude of the observed spectral shift is reasonable. However, it would be instructive to explore whether such a shift could result from the additional heating caused by the measured 23% decrease in electrical efficiency. This can be done by comparison with previously reported modeling and experimental data. The curves in Fig. 3 show that the optical power at 20 A has dropped 18.7 W by the end of the life test, and all this power is assumed to contribute to junction heating. While the heat sink temperature

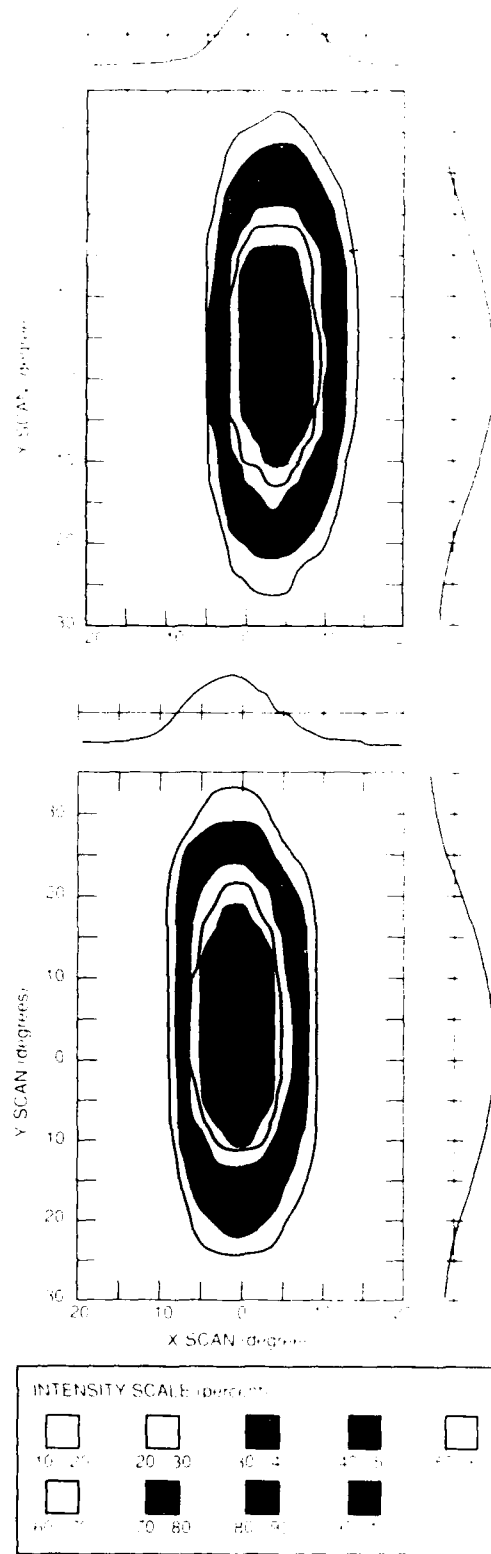


Fig. 5. Central region of the far field for the array on receipt (upper) and after  $3.6 \times 10^6$  shots (lower). Original is in color and the full scan range is  $\pm 45^\circ$ . The contour key is the same for both figures. The beam divergence is shown above and to the right of each pattern. The divergence plot traces the output intensity along the central axes, with the half-power points indicated by the intersection of the curve with the graph axis; each tick mark is  $5^\circ$ .

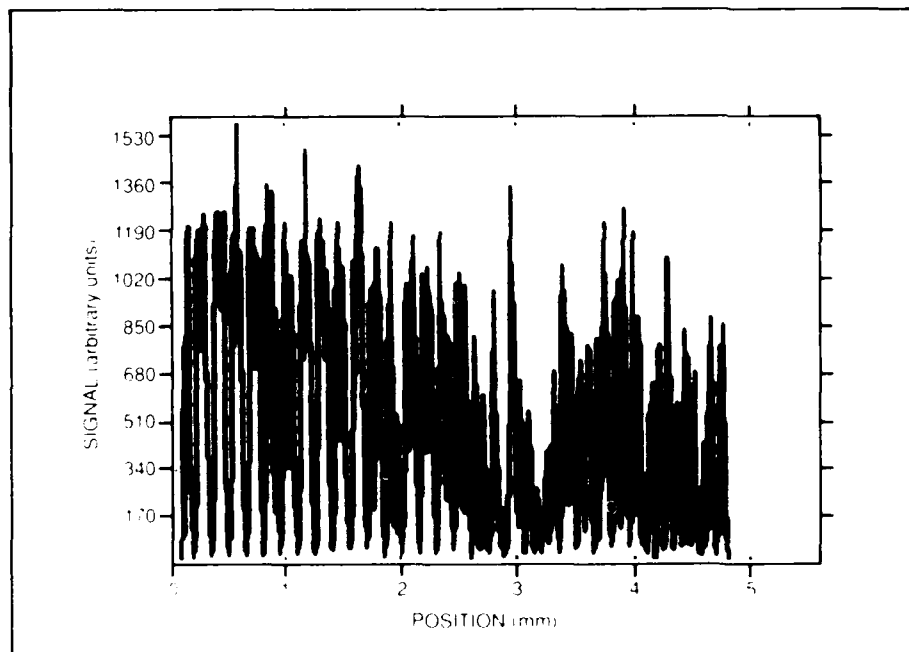
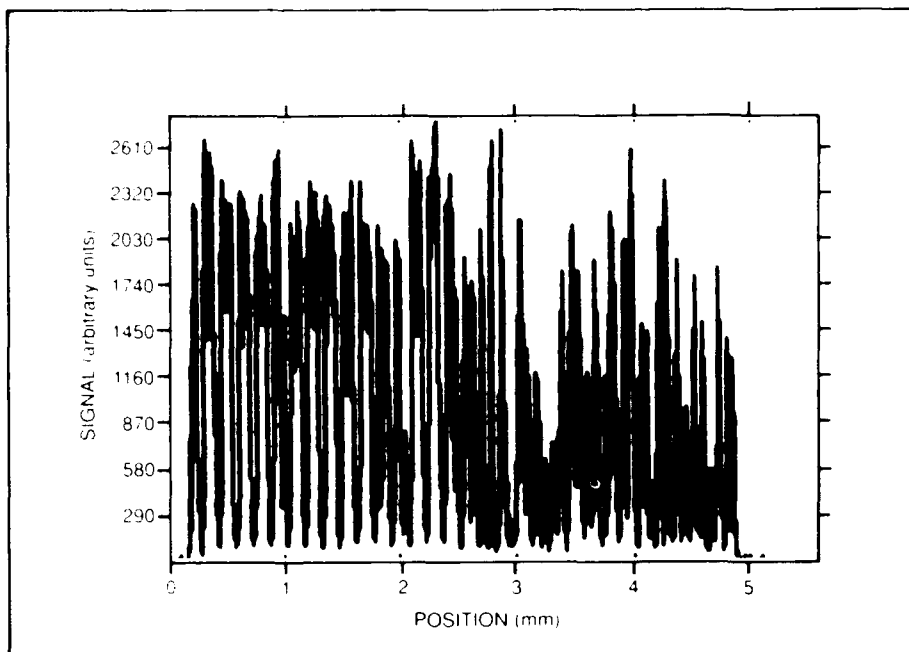


Fig. 6. Near field patterns of one of the ten bars in the 2-D array shown after  $3.6 \times 10^7$  (upper) and  $5.9 \times 10^7$  shots (lower). Each spike represents an individual stripe on the bar.

will not rise much due to the additional 0.1 W of average heat generated within the laser array, the transient temperature rise will be higher. Since the heat rise is initially confined to the junction,<sup>6</sup> the spectral shift (which depends only on the temperature of the active region) will be sensitive to additional transient heating. Suyama *et al.*<sup>7</sup> showed that for a low power buried heterostructure device the junction temperature reaches steady state after  $\sim 40 \mu\text{s}$ , but Streifer *et al.*<sup>8</sup> showed that for a linear array consuming 80 W/cm of waste heat the active region does not reach steady state temperature during a 600- $\mu\text{s}$  long pulse, and fur-

ther showed that heat is not effectively conducted to the heat sink during the first 200  $\mu\text{s}$ . Indeed, the temporal dependence of the wavelength for the linear bar shown in Fig. 2 confirms that steady state junction temperatures are not achieved during the first several hundred microseconds of the pulse.

The thermal resistance of several laser diode structures has been reported and ranges from 12 K/W for a 200-mW ten-stripe phased array<sup>9</sup> to 81 K/W for the buried heterostructure device.<sup>10</sup> Joyce and Dixon<sup>11</sup> have calculated the thermal resistance of a  $12 \times 375\text{-}\mu\text{m}$  heterostructure laser and shown that it varies be-

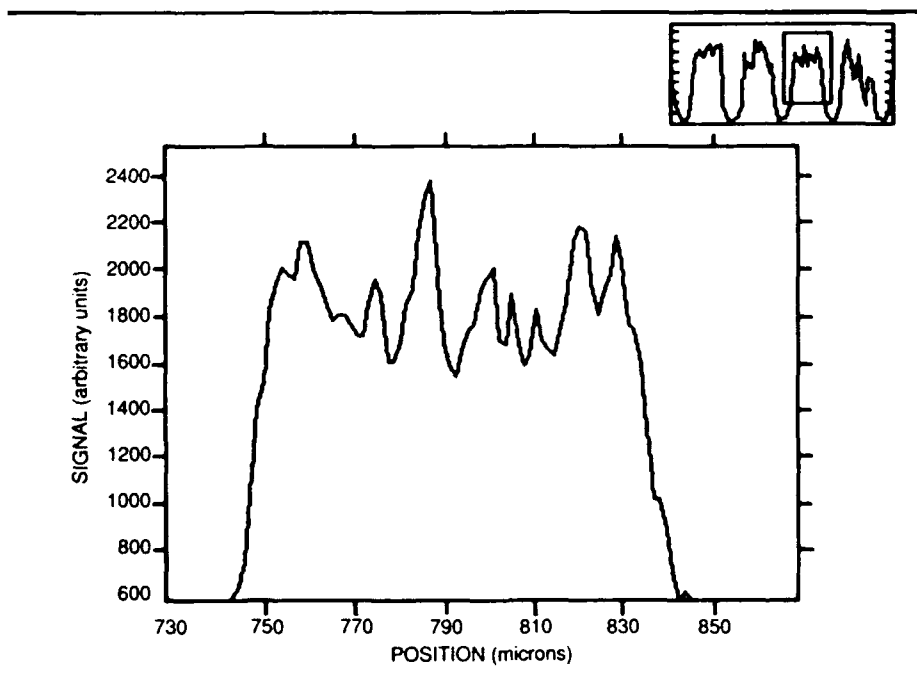
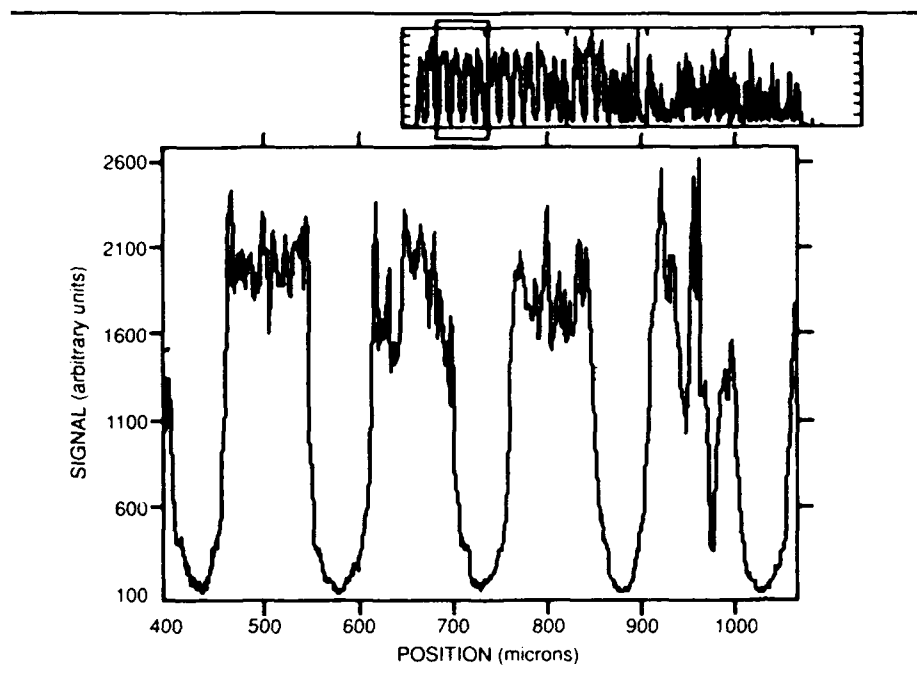


Fig. 7. Successive near field traces of the bar in Fig. 6 showing the zoom capability of the test facility software that allows expansion of a specific region of the near field pattern. The smaller trace in the upper right-hand corner of each near field shows a compressed version of the unexpanded near field pattern, with the rectangle indicating the area that is enlarged. For the upper trace the size of the rectangle is exaggerated for clarity. In the upper trace the intensity modulation across each mesa can easily be seen; in the lower trace the structure for a single mesa has been expanded.

between 14 K/W and 31 K/W depending on the thickness of the active and confinement layers. With 320 total stripes in the 2-D array, the incremental heating per stripe amounts to only 60 mW so that we would require a thermal resistance of  $\sim 165$  K/W to account for a 10 K increase (and hence a 3-nm shift) in each junction due to the additional excess heat. This is unlikely, particularly since the larger stripe dimensions of the GE diodes ( $100 \times 500 \mu\text{m}$ ) will have a reduced thermal

resistance compared to the above devices. We would expect at most a temperature rise of  $\sim 3$  K for each junction due to the combination of transient and steady state heating.

The magnitude of the observed spectral shift is larger than expected on the basis of the diode thermal resistivity alone, but may be accounted for by considering two additional effects. The first is that the assumed shift of 0.3 nm/K is only an approximation for

the composite spectrum of the array. It is not necessary (or likely) that the thermally induced spectral shift for the array results from each stripe shifting the same amount. Referring to Fig. 2(c) it can be seen that the time-integrated spectrum of the linear bar shows a good deal of intensity to the red of the peak, so that the composite peak could shift as a consequence of only a fraction of the stripes shifting to higher wavelength. While the spectra for the 2-D array do not show such a broad red wing, the individual stripes do not have uniform electrical and optical properties and will not equally generate the additional waste heat. Furthermore, efficiency of heat removal depends on the position of the stripe within the array. For example, in their analysis of thermal effects in phased arrays, Garmire and Tavis<sup>10</sup> calculated a large thermal nonuniformity across a 1-D array of stripes, with the highest temperature occurring at the center of the bar. The change of peak shape as the shot life increased, mentioned in discussing Fig. 4, is consistent with the concept that the emission from each of the stripes does not shift uniformly.

The second point to consider is that the lower optical power generated by the array at the end of the test is due primarily to a decrease in the slope efficiency rather than a threshold shift. Suyama *et al.*<sup>6</sup> have indicated that in general only one-half of the waste heat is consumed in the junction region while the rest heats the substrate, but the decreased slope efficiency is likely due to factors primarily affecting junction heating (free carrier absorption or quenching) and if this were the case all the excess heat would be localized at the junction. In the same context, it is possible that the aging of the stripes has caused an increase in the fraction of total waste heat deposited in the active region, thereby accelerating the spectral shift beyond that which could be accounted for due to the additional waste heat alone.

In any event, it seems clear from the data that thermal equilibrium is not achieved within the junction during the pulse, and based on the calculations in Ref. 7 the heat does not migrate to the heat sink prior to pulse termination. The resulting transient spectral shift is therefore not affected by the efficiency of the heat sinking. Both the near field and far field data were taken again with a commercially available beam diagnostic system<sup>11</sup> to evaluate and compare the same data, but the commercial system did not have adequate spatial resolution to be useful for the near field measurements. The system uses a video camera to record and digitize the image, and thus presents the data in a manner similar to that obtained from near field photographs. Since the dynamic range of the video detector is 100:1, saturation is an additional problem with this method. However, near field can be recorded in a shorter time than with the scanning technique used here, and such a system might be appropriate to use when speed is a primary consideration.

In summary, we have measured the effects of shot life on the spectrum, power vs current, near field, and far field patterns of a high power laser diode array.

We operated the array for  $5.9 \times 10^7$  shots at approximately half of its rated power and observed substantial (23%) degradation of the output power vs current, and a spectral shift of 3 nm. Presumably, had the array been tested at its full rated power the observed degradation would have been more severe. The power level used in this test was chosen to correspond to a power density of 1 kW/cm<sup>2</sup>. On the basis of the measurements reported in this work, we conclude that solid state laser device designs using high power diode array pumping must take the power degradation and spectral shift into account if efficient operation for 10<sup>7</sup> or more shots is desired. However, until the factors responsible for the measured degradation are understood and controlled, it is not realistic to expect extended operation from such devices. A point worth repeating is that the GE array tested is representative of what can currently be achieved in high power diode array manufacturing technology, and it is not our intention to detract from the capabilities of a specific manufacturer. On the contrary, we have tested a number of arrays from other manufacturers and have found this array to be superior in some aspects, and as good in others.

We wish to thank R. Solarz of Lawrence Livermore Laboratory for providing the laser diode array tested in this work.

## References

1. A. Rosen, *et al.*, "1 kW Peak Power 808 nm 2-D Laser Diode Array," *IEEE Phot. Tech. Lett.* **1**, 43-45 (1989).
2. P. S. Cross, G. L. Harnagel, W. Streifer, D. R. Scifres, and D. F. Welch, "Ultrahigh-Power Semiconductor Diode Laser Arrays," *Science* **237**, 1305-1309 (1987).
3. C. A. Krebs and B. D. Vivian, "High Power Quasi-CW and CW Laser Diode Bar Arrays," *Proc. SPIE* **893**, 35-37 (1988).
4. R. Scheps and J. Myers, "Laser Beam Diagnostic Facility (LBDF)," Naval Ocean Systems Center Technical Document Number 1257, Jan. 1989 (Naval Ocean Systems Center, Technical Information Division, Code 9613, San Diego, CA 92152).
5. A. Rosenberg, *et al.*, "High-Power High-Efficiency 770nm 2D Laser Diode Array," *Electron. Lett.* **24**, 1121-1122 (1988).
6. M. Suyama, N. Ogasawara, and R. Ito, "Transient Temperature Variation of Injection Lasers," *Jpn. J. Appl. Phys.* **20**, L395-L398 (1981).
7. W. Streifer, D. R. Scifres, G. L. Harnagel, D. F. Welch, J. Berger, and M. Sakamoto, "Advances in Diode Laser Pumps," *IEEE J. Quantum Electron.* **QE-24**, 883-894 (1988).
8. D. R. Scifres, R. D. Burnham, and W. Streifer, "High Power Coupled Multiple Stripe Quantum Well Injection Lasers," *Appl. Phys. Lett.* **41**, 118-120 (1982).
9. W. B. Joyce and R. W. Dixon, "Thermal Resistance of Heterostructure Lasers," *J. Appl. Phys.* **46**, 885-882 (1975).
10. E. M. Garmire and M. T. Tavis, "Heatsink Requirements for Coherent Operation of High-Power Semiconductor Laser Arrays," *IEEE J. Quantum Electron.* **QE-20**, 1277-1283 (1984).
11. Big Sky Software, Inc., Bozeman, MT 59722-3220.